Dynamic Analysis Modeling under Dynamic Eccentricity—Stator Inter-turn Fault Coupling with Design Technique for Reliability Rise of IPM-type BLDCM

Jin-Wook Reu[1], Jun-Kyu Park[1], Jin-Hur[1], *Senior Member IEEE*,
Byeong-Woo Kim[1], *Member IEEE* and Gyu-Hong Kang[2], *Senior Member IEEE*
[1]School of Electrical Eng., University of Ulsan, 102 Street Dae-hak, Nam-gu, Ulsan 680-749, Korea
[2]Korea Marine Equipment Research Institute, Busan, 1631-10, Korea
jinhur@ulsan.ac.kr

Abstract — In this paper, we have proposed a modeling technique for the classification of fault frequency components according to the fault state and the optimal rotor design for an increase in reliability and decrease in vibrations of an interior-type permanent magnet (IPM) motor. For minimizing the vibrations, optimal notches are designed. Fault states such as dynamic eccentricity fault, stator turn fault, and their coupling faults are modeled and analyzed using a nonlinear finite element method (FEM) and fast Fourier transform (FFT).

I. Introduction

Generally, the lifetime and reliability of an IPM motor are sharply decreased by mechanical vibrations [1]. In addition, these mechanical vibrations not only become the main cause for faults in the driving motor but also distort the controlled excitation current [1, 2]. In particular, a stator inter-turn fault (SITF), a type of electrical fault, is frequently generated by mechanical stress and thermal stress [1, 3]. SITF has caused a significant increase in the radial force and unbalanced magnetic force according to the simultaneous distortion of the air gap flux density and the input current. Therefore, generation of an SITF leads to a dynamic eccentricity fault (DEF). Moreover, when coupled faults (CFs) by combination of DEF and SITF occur, the generation of dynamic problems with additional vibration, noise, and torque pulsation increases considerably. From the viewpoint of fault detection and fault diagnosis, a classification of fault frequency components according to the fault type is essential for efficient fault response. However, the modeling technique for the classification of fault frequency components in an IPM motor having CFs has not been proposed in detail as yet.

In this paper, a modeling technique for the CFs analysis of DEFs with SITFs and a design technique for an IPM-type brushless DC motor (BLDCM) are proposed in order to obtain efficient fault response and vibration reduction.

II. Rotor Shape Design for Vibration Reduction

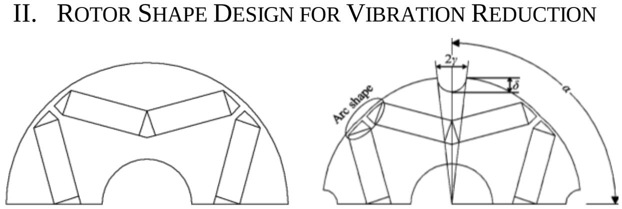

(a) Initial rotor (b) Notch-type rotor

Fig. 1. Initial rotor and designed notch-type rotor for vibration reduction

In order to balance the distribution of radial force and reduce the cogging torque, the rotor shape design is applied to notches [4]. Having an appropriate notch shape on the rotor pole face can help obtain a reduction in mechanical vibrations because of the reduction in the spatial 2nd harmonic with the influx of the spatial 3rd harmonic corresponding to the dispersion of the radial flux density caused by the notch. The initial model (4 poles and 6 slots) and the notch model for the reduction of the mechanical vibration of an IPM motor are shown in Fig. 1. The notch has a dead zone depth (δ) and a dead zone position (α) with a dead zone width (γ) of the radial flux density for the reduction of the spatial 2nd harmonic of the radial flux density. The analysis method of the cogging torque is used for the optimal design of these notches according to a space harmonic field analysis [4]. In addition, an arc shape is applied for the reduction of the cogging torque due to an increase in the air gap near the pole transition.

III. Modeling of Fault States

Fig. 2 presents the scheme of the proposed simulation model for the analysis of the fault frequency components and the electromagnetic vibration sources under CFs in an IPM motor. Fig. 3 presents the detailed section of the DEF and the SITF in CFs. In Fig. 3 (a), O_A is the center of the stator symmetry, O_B is the rotor rotation center, and O_R is the rotor symmetrical axis. Further, x and y represent the distance by which the rotor symmetrical axis is separated by the DEF. In this paper, the DEF is defined as follows: x, y = 0.35 [mm]. Under the DEF, the symmetry axis of the stator and the rotation axis of the rotor are identical, but the rotor symmetry axis fluctuates. In such a case, the air gap around the rotor is non-uniform and varies with time [5]. In Fig. 3 (b), *as1* and *as2* represent the healthy and the shorted turn, respectively, and i_f represents the circulating current in the shorted turns. R_f is the external impedance under the SITF. This model includes the shorted turn for the calculation of the circulating current induced by the variation of the magnetic flux linking the shorted turn.

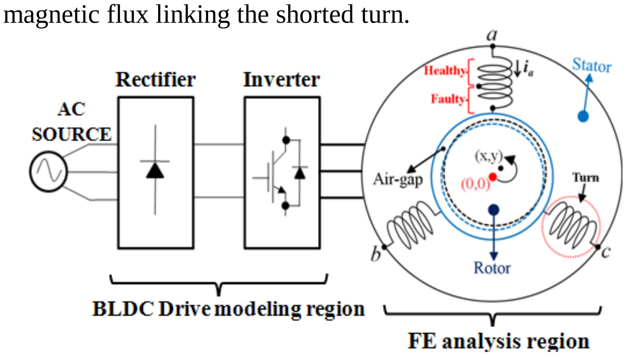

Fig. 2. Scheme of proposed FEM model with CFs

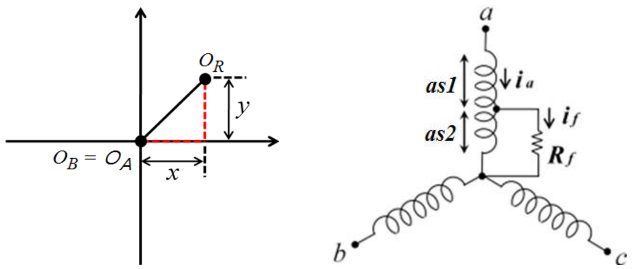

(a) Dynamic eccentricity fault (b) Stator inter-turn fault

Fig. 3. Schematic representation of DEF and SIFT

IV. Analysis and Results

The experimental sets for vibration measurement under a no-load condition are shown in Fig. 4. Fig. 5 shows the overall value of the tangential and radial components of vibration with respect to the rotating frequency. The vibration of the notch model is smaller than that of the initial model. Fig. 6 shows an analysis of the characteristics of the radial flux density in the air gap of notch model under the normal state and CFs, where the *Fr* of the SITF is applied at 25[%], the symbol *Fr*, which is referred to as the "fault fraction (*Fr*)", is defined as the ratio of the number of shorted turns to the number of turns per phase. Here, the CFs is a DEF coupled with an SITF (*Fr* = 25[%]). The coupling of a DEF and an SITF leads to an asymmetrical distribution of the radial flux density due to the non-uniformity of the air gap and an imbalance in the input current. This experiment used the Triaxial Accelerometer (x = 11.0[mV/G], y = 10.2[mV/G], z = 11.0[mV/G], Company name : Dytran, Model No. : 3023a).

Fig. 4. Equipment and machine for the vibration measurement

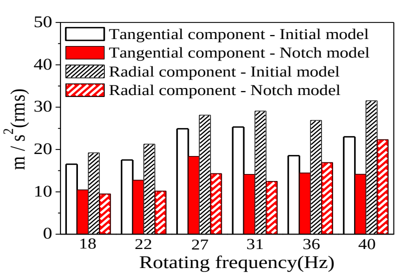

Fig. 5. Overall value of vibration with respect to rotating frequency

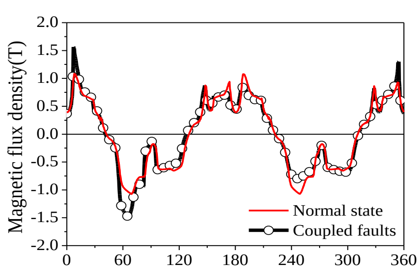

Fig. 6. Radial flux density in full-load IPM-type BLDCM air gap

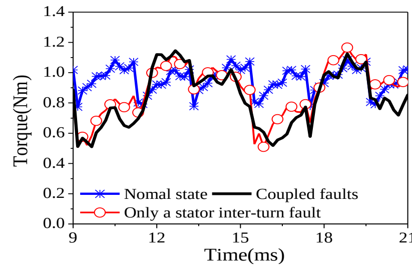

(a) Commutation torque under fault state

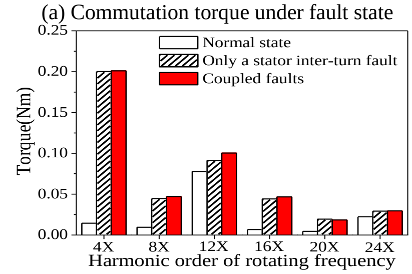

(b) Additional harmonic components caused by faults

Fig. 7. Commutation torque of notch model under various faults

Fig. 7 shows the additional harmonic components of the commutation torque and the commutation torque caused by various faults. In the case of only an SITF and CFs, integer multiples of the 4*X* component appear because the dependence of the circulating current on the PM of 4 poles is increased. Here, 12*X* and 24*X* are the innate components caused by a torque ripple and the cogging torque. Here, *X* denotes a rotation frequency of 40 [Hz]. Maxwell software was used for the FEM analysis.

V. Conclusion

In this paper, a modeling technique for the CFs analysis and a design technique for an IPM-type BLDCM are proposed in order to obtain efficient fault response and vibration reduction. The rotor shape design for notches bring about balance to the distribution of radial force and reduce the cogging torque. In addition, the harmonics component of the commutation torque analysis in event of the fault can help to detect the type of fault.

This work was supported by the development program of local science park funded by the ULSAN Metropolitan City and the MEST(Ministry of Education, Science and Technology)

VI. References

[1] H. S. Ko and K. J. Kim, "Characterization of Noise and Vibration Sources in Interior Permanent-Magnet Brushless DC Motors", *IEEE Trans. on Magn.*, vol. 40, no. 6, pp. 3482–3489, Nov. 2004.

[2] Z. Q. Zue, D. Ishak, D. Howe and J. Chen, "Unbalanced Magnetic Forces in Permanent Magnet Brushless Machines With Diametrically Asymmetric Phase Windings", *IEEE Trans. Ind. Appl.*, vol. 43, no. 6, pp. 1544–1553, Nov/Dec. 2007.

[3] J. H. Yun, K. H. Lee, K. W. Lee, S. B. Lee and J. Y. Yoo, "Detection and Classification of Stator Turn Faults and High-Resistance Electrical Connections for Induction Machines", *IEEE Trans. Ind. Appl.*, vol. 45, no. 2, pp. 666–675, Mar/Apr. 2009.

[4] G. H. Kang, Y. D. Son, G. T. Kim and J. Hur, "The Novel Cogging Torque Reduction Method for Interior Type Permanent Magnet Motor", *IEEE Trans. Ind. Appl.*, vol. 45, no. 1, pp. 161–167, Jan. 2009.

[5] B. M. Ebrahimi, J. Faiz, and M. J. Roshtkhari, "Static-, Dynamic-, and Mixed-Eccentricity Fault Diagnoses in Permanent-Magnet Synchronous Motors", *IEEE Trans. Ind. Appl.*, vol. 56, no. 11, pp. 4727–4739, Nov. 2009.